Environment Protection Engineering

Vol. 22 1996 No. 1–2

MARIA T. MARKIEWICZ*

THE MULTIBOX REACTIVE PLUME MODEL WITH VARIABILITY OF METEOROLOGICAL PARAMETERS TAKEN INTO ACCOUNT. PART II. SIMULATION OF THE BEHAVIOUR OF REACTIVE PLUME

Application of the reactive plume model (MRPM) to simulation of the behaviour of a reactive plume emitted from a single, high-level point source, formulated in part I of this paper, is described. The behaviour of the reactive plume in the summer with sunshine and warm weather is analysed. Three stages typical of the ageing plume observed in the field experiments are reproduced by the model. The model predictions of key pollutants indicate that MRPM model can simulate the photochemical processes in the reactive plumes.

1. INTRODUCTION

Part I of this paper [4] presents the multibox reactive plume model (MRPM) formulated for the simulation of the behaviour of reactive pollutants emitted from a single, high-level point source. The model developed allows us to take into account change of meteorological conditions in time.

This part describes the results of computer simulations carried out using the MRPM model. The behaviour of the reactive plume emitted from a fossil fuel-burned electric power station during the summer with sunshine and warm weather is considered. The plume evolution is analysed in connection to primary pollutants (like sulphur dioxide, nitrogen oxides), radicals (like OH, HO_2) and secondary pollutants (like ozone, PAN).

First, input data applied are described. Next, the results of the model calculations for key species are discussed.

*Technical University of Warsaw, Department of Environment Engineering, Institute of the Systems of Environment Engineering, ul. Nowowiejska 20, 00-653 Warszawa, Poland.

2. DESCRIPTION OF INPUT DATA

Simulations of the behaviour of the reactive plume emitted from a high-level point source have been carried out for a chosen scenario. In this scenario, meteorological data represent typical conditions during the so-called 'ozone episode day', i.e. when high-level ozone concentrations are observed. Parameters of stack emission correspond to a power plant of a medium size. Emissions of pollutants from ground level sources are equal to average emissions of these species for UK.

In this paper, detailed results of one numerical experiment are presented. The plume evolution is traced for 11 hours starting from 7 a.m.

During this time the meteorological conditions change from slightly stable (Pasquil stability class 3) through very unstable to slightly stable again. The wind velocity, temperature and depth of the mixing layer increase gradually. The detailed meteorological data are shown in table 1.

Table 1

Meteorological data for the scenario chosen for the study

Hour of the day	Depth of the mixing layer [m]	Wind velocity [m/s]	Ambient temperature [°C]	Atmospheric stability class*
7.00	425	1.85	18.18	3
8.00	550	2.01	19.33	2
9.00	675	1.85	20.60	2
10.00	800	2.48	21.92	2
11.00	925	2.75	23.19	1
12.00	1050	3.02	24.32	1
13.00	1175	3.27	25.24	1
14.00	1300	3.48	25.89	2
15.00	1300	3.65	26.22	2
16.00	1300	3.75	26.20	2
17.00	1300	3.79	25.85	3
18.00	1300	3.75	25.17	3

*Classes of atmospheric stability: 1 – very unstable, 2 – unstable, 3 – slightly unstable, 4 – neutral, 5 – slightly stable, 6 – stable.

In order to illustrate how the change of meteorological conditions in time affects the plume evolution, an additional run of the model has been carried out. In this additional run, the meteorological parameters independently of the depth of the mixing layer have been kept constant during the time of plume travel and we obtain the values from the time when pollutants were injected from the stack to the atmosphere.

The stack emission data are presented in table 2. The data include: the height of the stack, its diameter, velocity and temperature of gases at the stack exit, intensity of the emissions of NO, NO_2 and SO_2.

Table 2

Emission parameters of the stack used in the numerical experiment

Parameter	Value	Units
Emission intensity of		
SO_2	$1.29 \cdot 10^{25}$	molecule/s
NO	$4.34 \cdot 10^{24}$	molecule/s
NO_2	$2.17 \cdot 10^{23}$	molecule/s
Stack height	100	m
Stack diameter	6	m
Gas velocity	5	m
Gas temperature	420	K

The emission data for ground level sources used are taken after DERWENT [2]. It is considered that the ground level sources emit the following species: CO, NO_x, SO_2 and hydrocarbons.

At the start of the model run the initial concentrations of the pollutants in the ambient air have been added to the values determined in a separate model run. This model run started at 6.00 a.m. from the unpolluted tropospheric background concentrations (50 ppbv of O_3, 2 ppbv of NO, 6 ppbv of NO_2, 1700 ppbv of CH_4 and 120 ppbv of CO). The pollution has been traced for more than 24 hours [5].

The initial concentrations of SO_2, NO and NO_2 in the plume have been calculated based on the stack emissions.

3. RESULTS AND DISCUSSION

The results of the model calculations presented here include the following species: SO_2, NO, NO_2, O_3, PAN, OH, HO_2 and RO_2. Such gases as SO_2 and NO represent typical primary pollutants emitted from a stack. Concentrations of O_3, PAN and NO_2 indicate the amount of photochemical oxidants which have been produced; however, NO_2 in a small amount is also emitted from the stack. Concentrations of radicals indicate the potential for further hydrocarbon degradation. RO_2 represents here the summa of radicals such as HO_2, CH_3O_2, CH_3COO_2 and $C_2H_5O_2$.

The results are presented in two ways. Either the concentrations of species in the plume and ambient air are shown as a function of time, or the distributions of species across the plume are presented at different times of the ageing plume.

In the simulations described, the plume cross section is represented by 20 boxes. Due to the symmetry of the plume the concentrations of the species are calculated only in 10 boxes. The eleventh box represents the concentration of species in the ambient air.

The results of the basic numerical experiment, in which meteorological parameters vary in time during the plume transport, are presented in figures 1–17.

The concentrations of SO_2 are shown in figures 1 and 2. The plots representing the distribution are typical of primary pollutants. The concentration of SO_2 in the plume decreases with the travel time. Initially the concentrations of species in the plume axis exceed greatly the ambient values and the distribution of concentration follows the hat-like profile. After approximately 10 hours of travel, the concentrations in the plume lessen to the ambient values.

The concentrations of NO are shown in figures 3 and 4. The distribution of NO concentrations follows the pattern of SO_2 described above.

Figures 5 and 6 present the distribution of NO_2 concentration in time. Initially the highest concentration of NO_2 is in the plume axis and the hat-like profile is observed. With the time, due to chemical production of NO_2, the concentration of NO_2 rises quickly in the plume cross section. The concentration peaks first at the plume boundaries; however, the maximum value is observed in the plume axis and it appears after one hour of plume travel.

Figure 7 demonstrates the fractions of NO and NO_2 concentrations in total NO_x as a function of time. The values represent average concentrations in the plume. Initially NO concentration represents 95% of the total NO_x concentration. After approximately 11 hours of plume travel the fractions of NO and NO_2 concentrations are 7% and 93%, respectively.

Figures 8 and 9 show the distribution of OH with time. Here the concentrations in the plume also depend on the stage of plume development. The initial deficit of OH is built up gradually with time. The excess of OH concentration in the plume axis peaks after less than 5 hours of travel.

The concentrations of HO_2 are shown as a function of time in figures 10 and 11. The HO_2 behaviour is also related to the stage of the plume development. There is a shift in peak of HO_2 in comparison to OH. The peak of HO_2 concentration appears after approximately 7.5 hours of transport.

The calculated temporal behaviour of RO_2, which is a summa of different radicals, is illustrated in figures 12 and 13. The distribution of RO_2 resembles very much HO_2 distribution. However, in this case, the concentration of RO_2 in the plume does not exceed its concentration in the ambient air.

The O_3 concentrations are shown in figures 14 and 15. The distribution of O_3 is typical of secondary pollution. Initially there is ozone depletion in the plume, with the minimum in the plume axis. The O_3 concentrations rise with the travel time. An excess of ozone first is generated near the plume boundaries. It advances towards the plume centreline gradually. The ozone concentration in the plume axis peaks after 6 hours of transport. It rises by 12.5 % above the background ozone level.

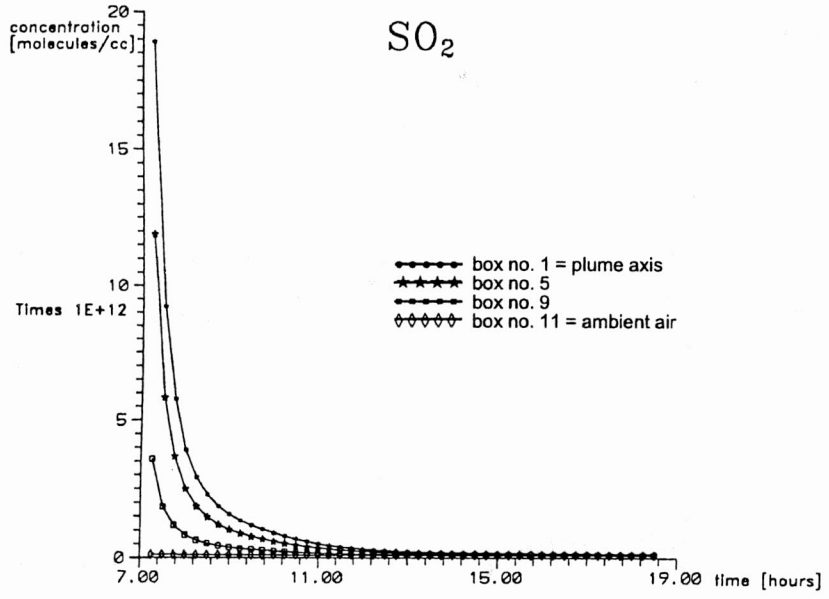

Fig. 1. SO_2 concentration for the chosen individual plume box and ambient air as a function of time

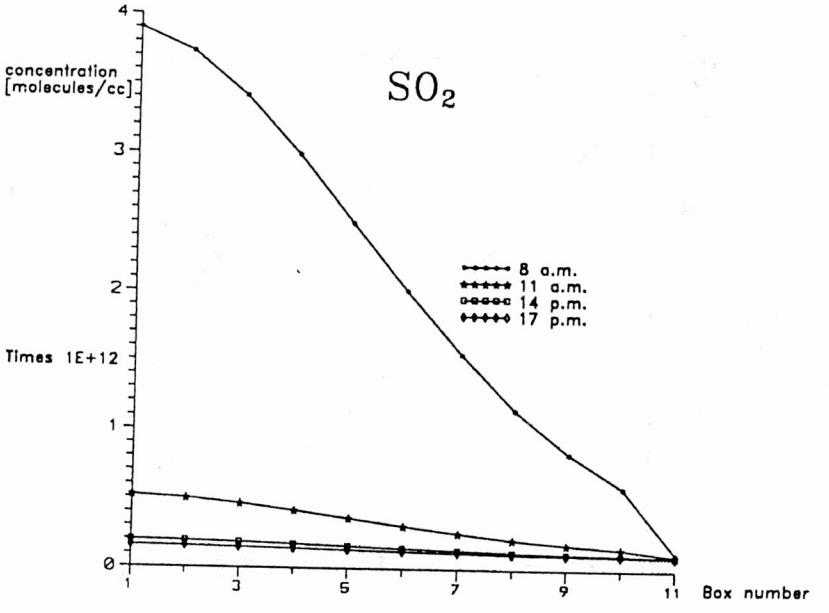

Fig. 2. Distribution of SO_2 concentration across the plume at different times.
The pollutant was emitted from the stack at 7 a.m.
The concentrations calculated in the plume axis
and ambient air correspond to boxes no. 1 and 11, respectively

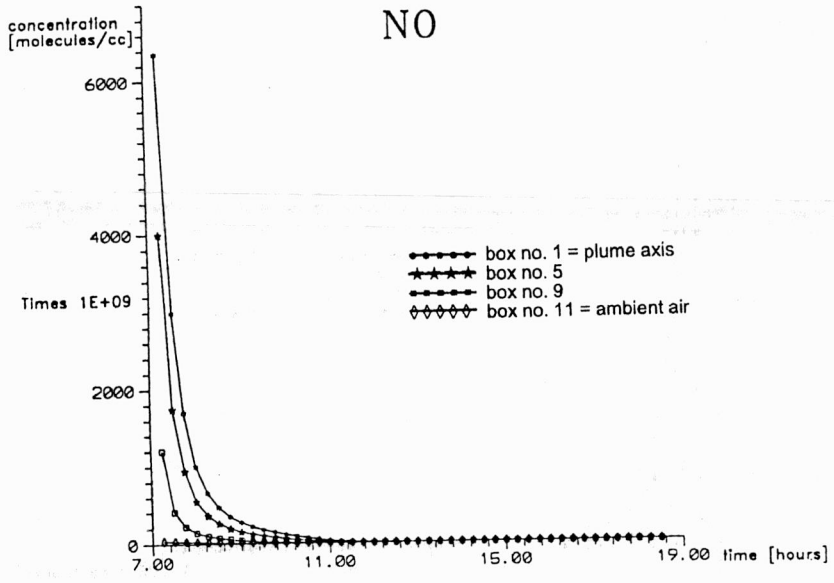

Fig. 3. NO concentration for the chosen individual plume box and ambient air as a function of time

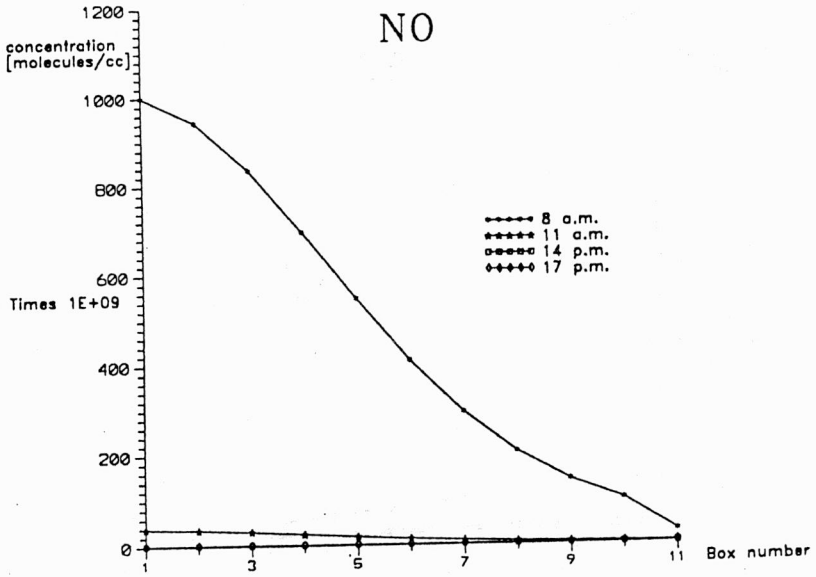

Fig. 4. Distribution of NO concentration across the plume at different times.
The pollutant was emitted from the stack at 7 a.m.
The concentrations calculated in the plume axis
and ambient air correspond to boxes no. 1 and 11, respectively

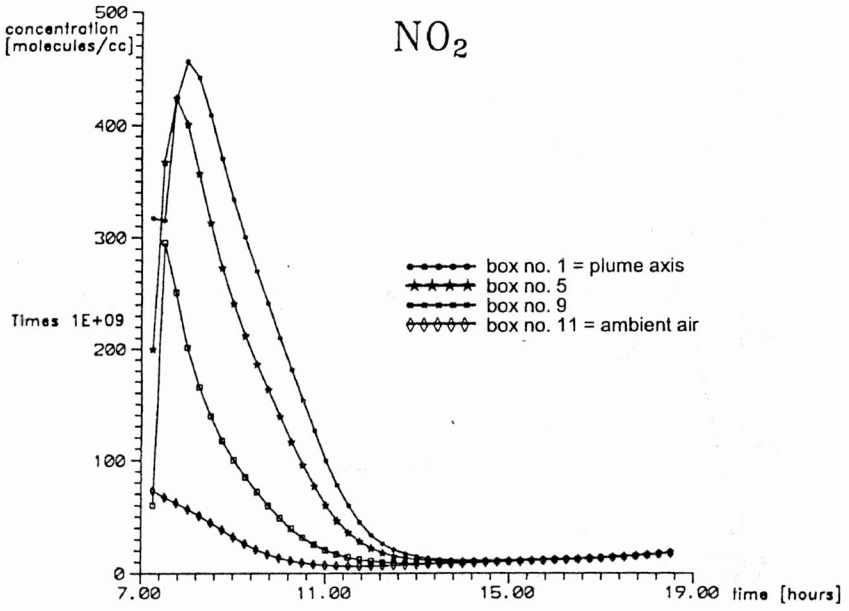

Fig. 5. NO_2 concentration for the chosen individual plume box and ambient air as a function of time

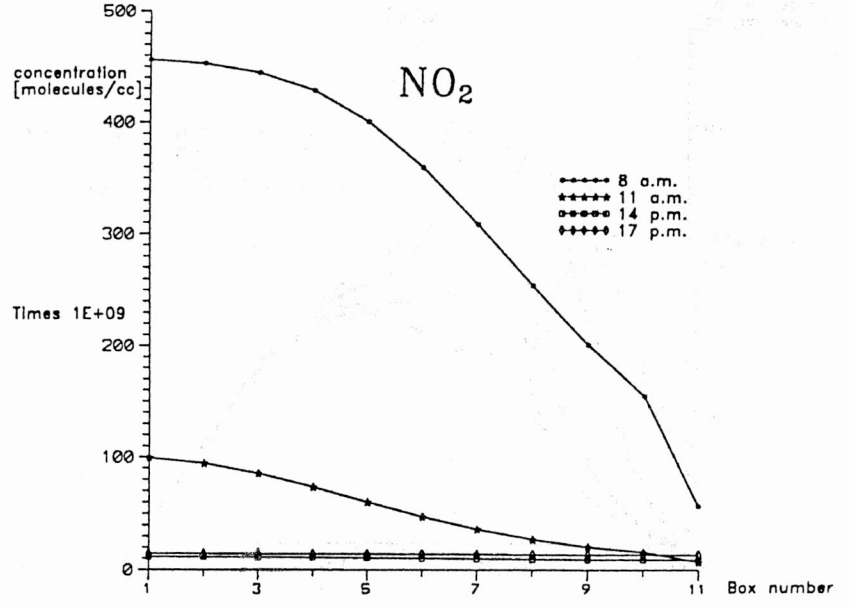

Fig. 6. Distribution of NO_2 concentration across the plume at different times. The pollutant was emitted from the stack at 7 a.m. The concentrations calculated in the plume axis and ambient air correspond to boxes no. 1 and 11, respectively

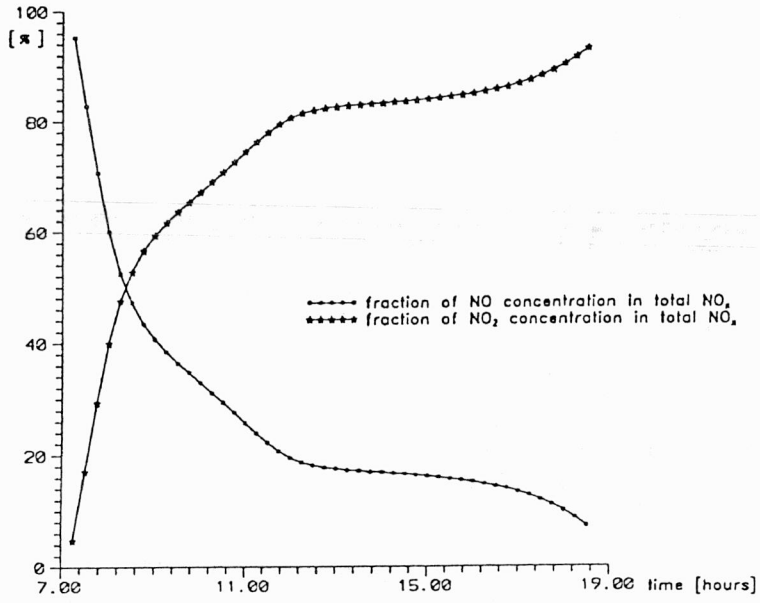

Fig. 7. Fractions of NO and NO_2 concentrations in total NO_x as a function of time

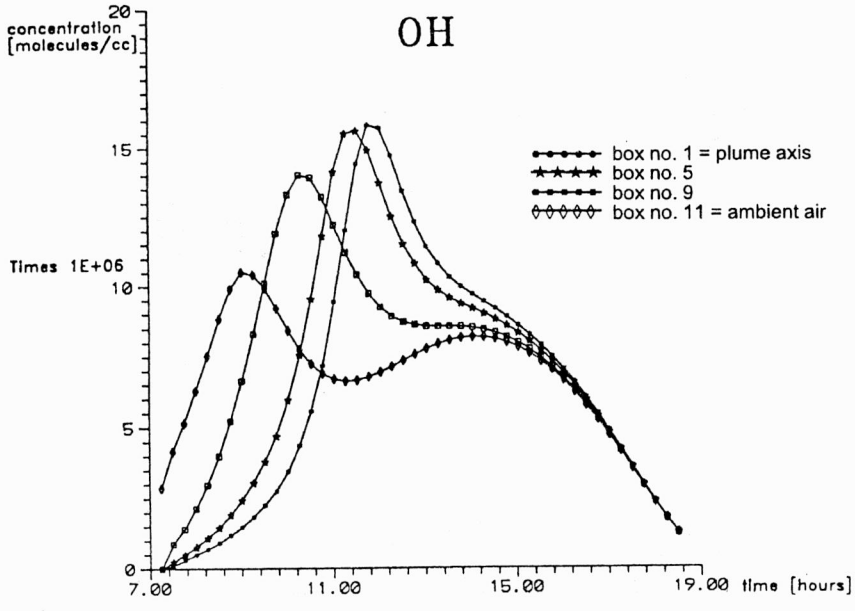

Fig. 8. OH concentration for the chosen individual plume box and ambient air as a function of time

The calculated temporal behaviour of PAN is illustrated in figures 16 and 17. It follows the pattern of O_3 described above.. The peak value of PAN concentration in

the plume axis is reached after approximately 6.5 hours of travel time. The excess of PAN concentration is equal to 8.4 % of the ambient value.

The results of the basic model run have been compared with the results of additional model run in which meteorological conditions have been kept constant (independently of the depth of the mixing layer). The relative difference between the plume axis concentrations obtained for the basic and additional model runs are shown in table 3. Each value has been calculated as a difference between the concentrations from additional run and basic one divided by the basic simulation concentration multiplied by 100.

The discrepancies in the plume axis in these two cases vary with the distance from the stack, i.e. with the plume travel time and for the individual species.

Table 3

Relative differences between the plume axis concentrations of SO_2 and PAN for the 2 cases studied which differ in a treatment of meteorological conditions*

Time [hour]	SO_2 [%]	PAN [%]
7^{15}	0	0
8	32	–24
9	48	–24
10	53	–27
11	74	–42
12	109	–48
13	117	–38
14	105	–18
15	97	–7
16	91	–1
17	83	1
18	76	2

*These values are calculated as the difference between the concentration from the additional run and basic one divided by the basic simulation concentration.

For SO_2 the predicted concentrations in the additional run are higher than the basic run concentrations (except of the initial value). The relative difference reaches the highest value of 117% after approximately 6 hours of travel from the stack.

For PAN the concentrations in the additional run are generally lower than the concentrations in the basic simulation. The discrepancy reaches –48% at the fifth hour of plume travel.

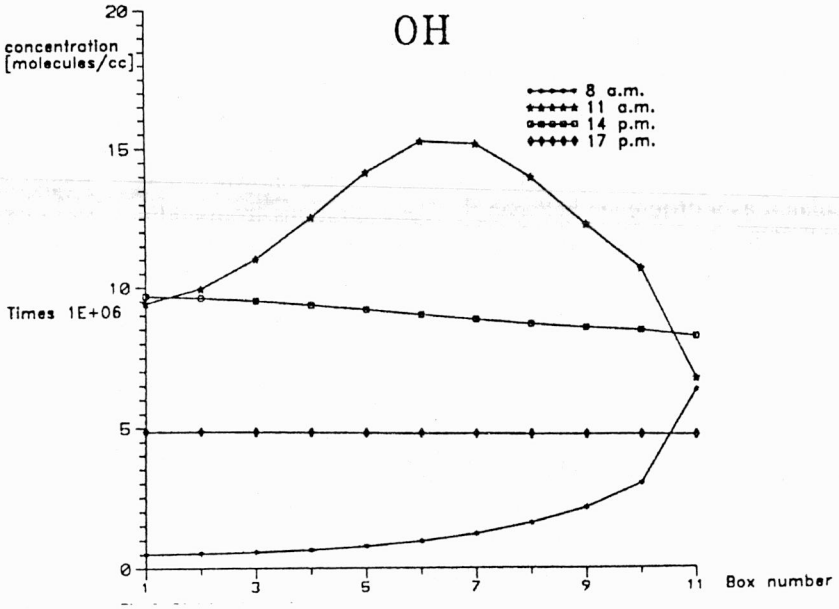

Fig. 9. Distribution of OH concentration across the plume at different times. The pollutant was emitted from the stack at 7 a. m. The concentrations calculated in the plume axis and ambient air correspond to boxes no. 1 and 11, respectively

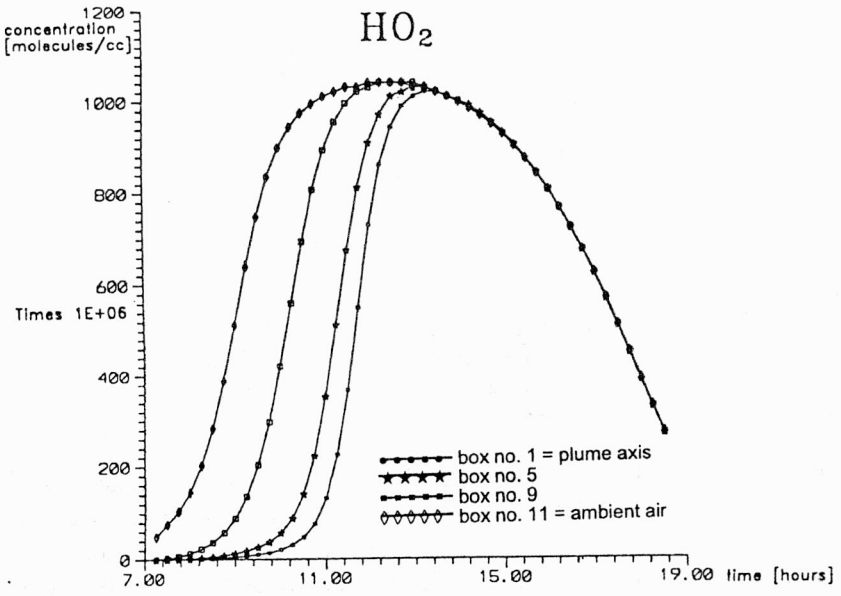

Fig. 10. HO_2 concentration for the chosen individual plume box and ambient air as a function of time

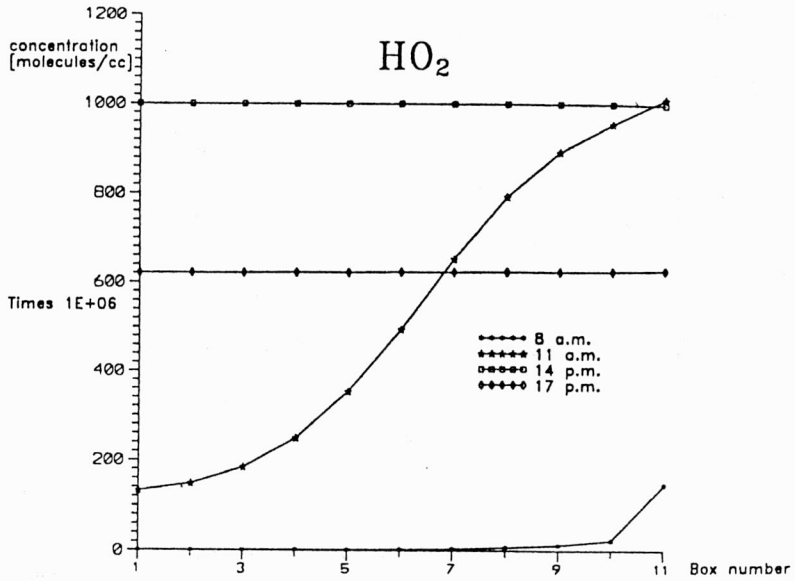

Fig.11. Distribution of HO_2 concentration across the plume at different times. The pollutant was emitted from the stack at 7 a.m. The concentrations calculated in the plume axis and ambient air correspond to boxes no. 1 and 11, respectively

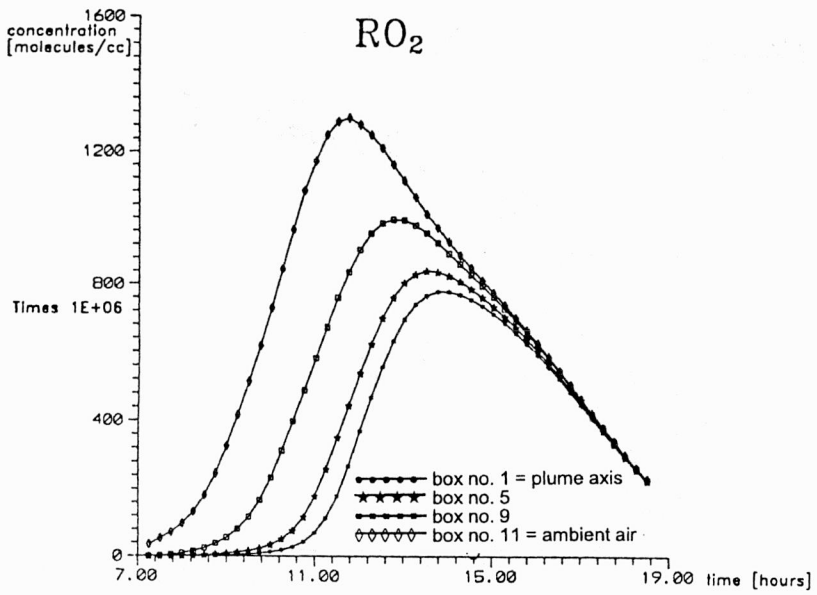

Fig. 12. RO_2 concentration for chosen individual plume box and ambient air as a function of time

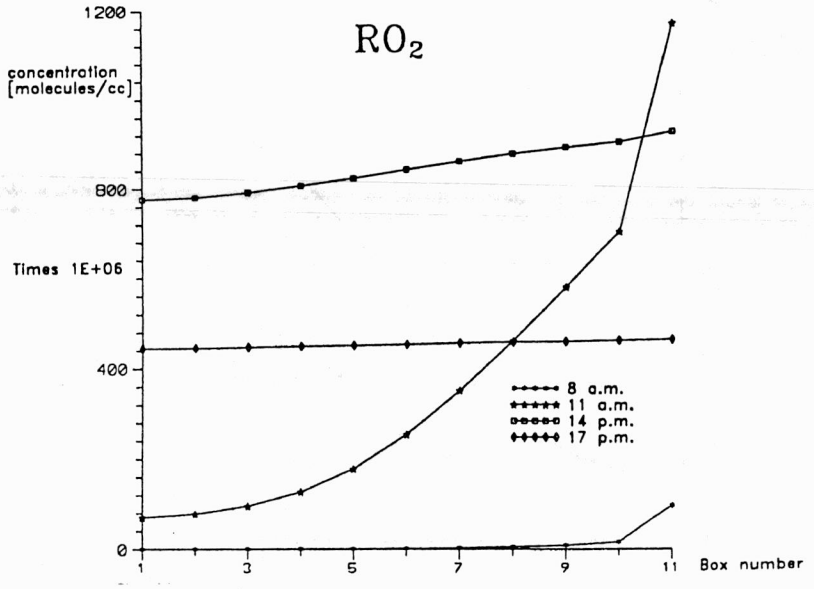

Fig.13. Distribution of RO_2 concentration across the plume at different times. The pollutant was emitted from the stack at 7 a.m. The concentrations calculated in the plume axis and ambient air correspond to boxes no. 1 and 11, respectively

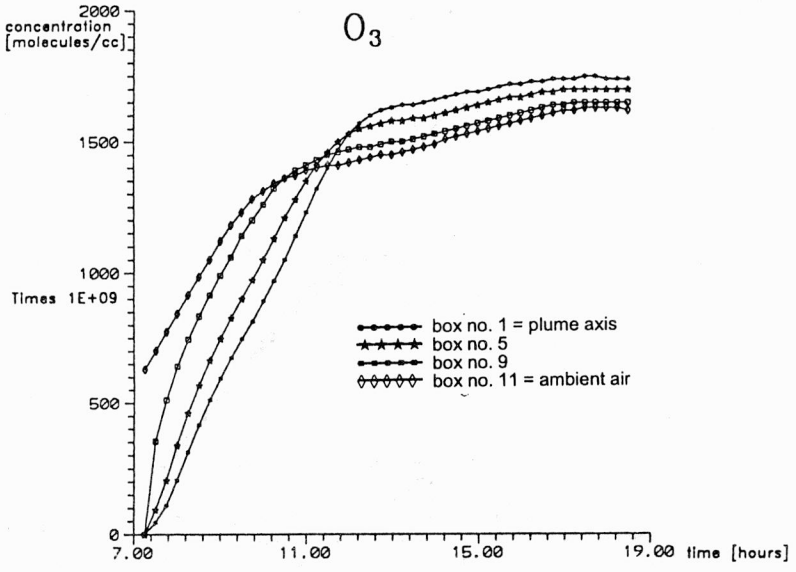

Fig. 14. O_3 concentration for the chosen individual plume box and ambient air as a function of time

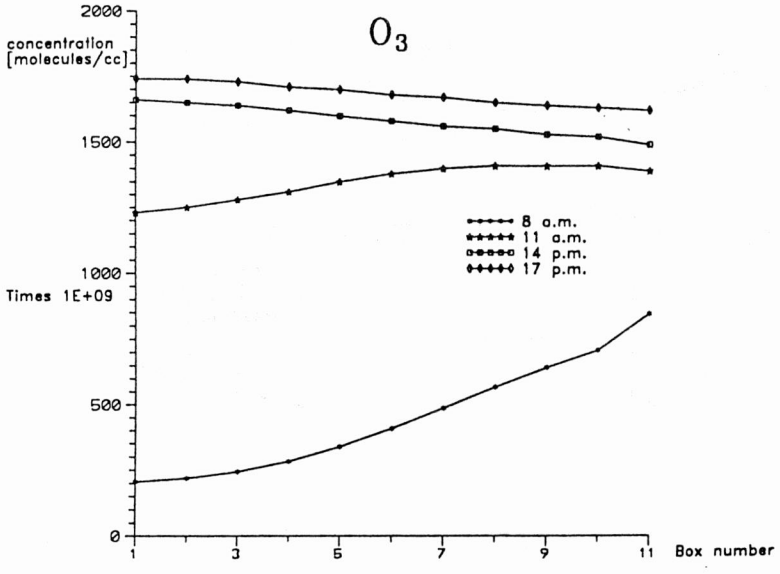

Fig.15. Distribution of O_3 concentration across the plume at different times. The pollutant was emitted from the stack at 7 a.m. The concentrations calculated in the plume axis and ambient air correspond to boxes no. 1 and 11, respectively

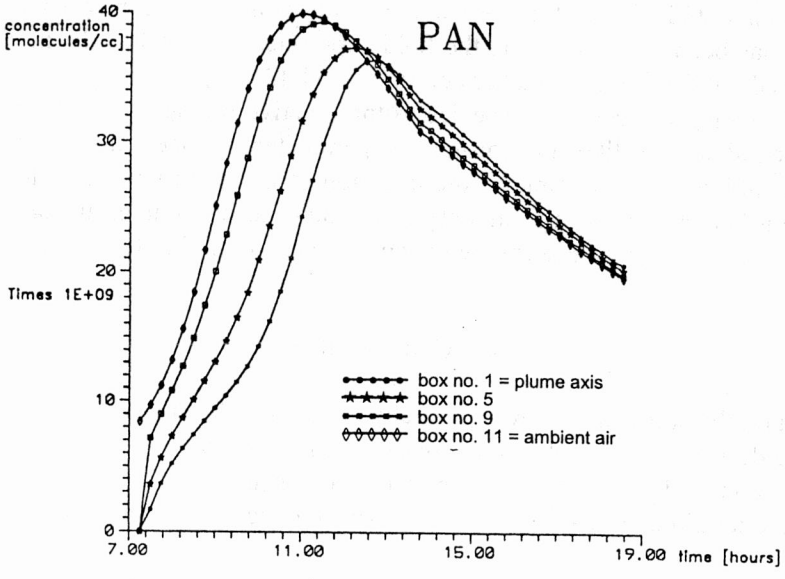

Fig. 16. PAN concentration for the chosen individual plume box and ambient air as a function of time

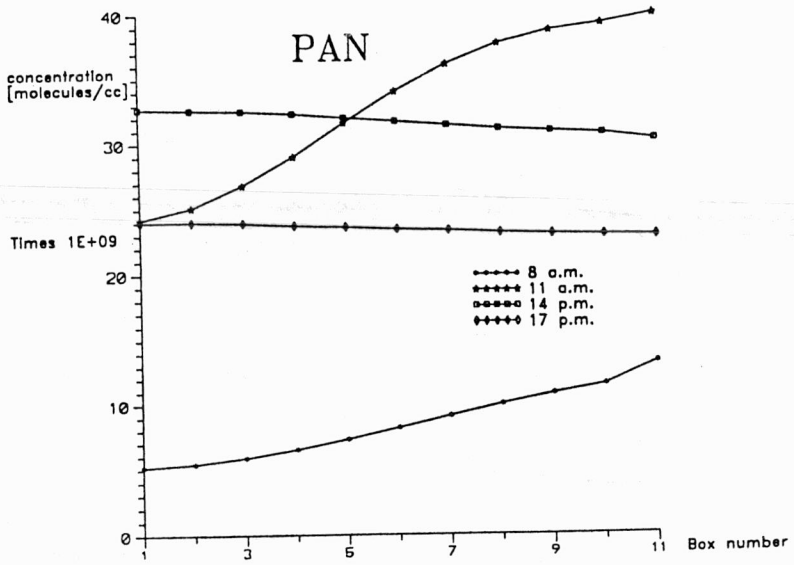

Fig. 17. Distribution of PAN concentration across the plume at different times. The pollutant was emitted from the stack at 7 a.m. The concentrations calculated in the plume axis and ambient air correspond to boxes no. 1 and 11, respectively

The described above characteristics of the reactive plume evolution is typical of the conditions studied, i.e. for the summer with sunshine and warm weather. This statement has been made based on the field experiments as well as the model simulations carried out for the fair weather conditions [1], [3], [6].

The formation of secondary species in the reactive plumes depends on the set of environmental factors like: meteorological parameters, concentrations of species in the plume and ambient air, time of the injection of the stack pollutants to the atmosphere. Further studies on the modelling of the reactive plumes using the MRPM model for a wide range of environmental conditions will probably be undertaken.

4. CONCLUSIONS

Based on the study the following conclusions can be formulated:

1. The described above characteristics of the reactive plume evolution is typical of the conditions studied, i.e. for the summer with sunshine and warm weather. The results of model simulations are consistent with the field observations of power plant plumes.

2. The results of the simulations of the evolution of the reactive plume carried out using the MRPM model for the chosen scenario show significant differences in distributions of concentrations for primary and secondary pollutants.

3. In the case of primary pollutants, for example SO_2, the slow decay of concentration with prolonging the time of transport is predicted. In the plume cross section, the maximum concentrations are observed in the plume axis.

4. In the case of secondary pollutants, for example O_3 or OH radical, the crucial dependence of distribution of species on plume stage development is observed. Three stages of the plume development are distinguished: the initial stage with depletion and minimum concentration at the plume centreline, the intermediate stage with active fringe region and centreline chemistry lagged behind, and the fully developed stage with maximum concentration at the plume centreline.

5. The comparison of the results obtained for the basic model run and additional run, which differ in the treatment of meteorological conditions, shows that in modelling the reactive plumes on a mesoscale it is important to consider the change of meteorological conditions in time.

6. Further studies on modelling the reactive plumes using the MRPM model for a wide range of environmental conditions would be useful. However, model predictions of key pollutants indicate that the model developed can simulate the photochemical processes in the reactive plumes.

REFERENCES

[1] DAVIS D.D., SMITH G., KLAUBER G., *Trace gas analysis of power plant plumes via aircraft measurements: O_3, NO_x, SO_2 chemistry*, Science, 1974, 186, 733–36.

[2] DERWENT R.G., *Computer modelling studies of photochemical air pollution formation in power station plumes in the United Kingdom*, AERE Report R-10631, AEA Technology, Harwell Laboratory,1981.

[3] Hov O., ISAKSEN J.S.A., *A chemical model for urban plumes: test for ozone and particulate sulphur formation in St. Louis urban plume*, Atm. Env., 1978, 12, 599–604.

[4] MARKIEWICZ M., *The multibox reactive plume model with variability of meteorological parameters taken into account.* Part I. *Model formulation*, Env. Prot. Eng., 1996, Vol. 22, No. 1, 2, pp. 39–55.

[5] MARKIEWICZ M., *The multibox reactive plume model with variability of the emission and meteorological parameters taken into account*, AEA Technology, Harwell Laboratory Report, 1994.

[6] STEWARD D.A., LIU M.K., *Development and application of a reactive plume model*, Atm. Env.,1981, 15, 2377–2393.

WIELOPUDEŁKOWY MODEL SMUGI REAKTYWNEJ CHEMICZNIE UWZGLĘDNIAJĄCY ZMIENNOŚĆ WARUNKÓW METEOROLOGICZNYCH. CZĘŚĆ II. SYMULACJA ZACHOWANIA SMUGI REAKTYWNEJ CHEMICZNIE

Przedstawiono wyniki symulacji zachowania się reaktywnej smugi emitowanej z punktowego źródła emisji za pomocą wielopudełkowego modelu. Podstawy teoretyczne modelu opisano w pierwszej części tego artykułu. Analizowano zachowanie się smugi w słoneczny, ciepły, letni dzień. Wyniki symulacji są zgodne z obserwacjami smug emitowanych z rzeczywistych kominów. Widoczne są trzy etapy w ewolucji smugi.